Supplementary Material:

Effect of Dissolved KOH and NaCl on the Solubility of Water in Hydrogen: A Monte Carlo Simulation Study

Parsa Habibi,[1,2] Poulumi Dey,[2] Thijs J. H. Vlugt,[1] and Othonas A. Moultos[1, a)]

[1)] *Engineering Thermodynamics, Process & Energy Department, Faculty of Mechanical Engineering, Delft University of Technology, Leeghwaterstraat 39, 2628 CB Delft, The Netherlands*

[2)] *Department of Materials Science and Engineering, Faculty of Mechanical Engineering, Delft University of Technology, Mekelweg 2, 2628 CD Delft, The Netherlands*

(Dated: 5 July 2024)

[a)] Electronic mail: o.moultos@tudelft.nl

Derivation of the relation between the excess chemical potential (i.e., with respect to the ideal gas reference state) and the second virial coefficient in the gas phase (Section S1); Computed solubilities of the Marx H_2 force field[1] in TIP4P/μ water (discussed in the Supporting Information of Ref.[2]) force field (Figure S1); Force field parameters (Tables S1-S5); Number of molecules used in CFCMC simulations (Tables S6-S7); Raw data tables for the Vapor-Liquid Equilibria of H_2 and aqueous KOH and NaCl solutions (Tables S8-S13).

S1. DERIVATION OF RELATION BETWEEN GASEOUS EXCESS CHEMICAL POTENTIALS AND THE SECOND VIRIAL COEFFICIENT

We derive an equation relating the excess chemical potential of species i in the gas phase ($\mu^{\mathrm{ex}}_{\mathrm{G},i}$) to the second virial coefficient (pressure expansion) of the pure gas of species i ($B_{2P,i}$). The equation derived in this section is applied to a single component (pure) solution of water vapor in Section III.B of the main text.

The excess chemical potential of component i in the gas phase, $\mu^{\mathrm{ex}}_{\mathrm{G},i}$, is related to the the fugacity coefficient (ϕ_i) of species i via[3]:

$$\mu^{\mathrm{ex}}_{\mathrm{G},i} = RT \ln\left(\frac{y_i \phi_i PV}{RT n_i}\right) \tag{S1}$$

where R is the gas constant, T is the temperature (in units of K), y_i is the mole fraction of species i in the gas phase, P is the total pressure (in units of Pa), V is the total volume (in units of m^3), and n_i is the total number of moles of species i. Eq. S1 is derived in the Supporting Information of Ref.[3] As $y_i = n_i/n_{\mathrm{t}}$ (where n_{t} is the total number of moles in the gas phase), Eq. S1 can be simplified:

$$\mu^{\mathrm{ex}}_{\mathrm{G},i} = RT \ln\left(\frac{n_i \phi_i PV}{n_{\mathrm{t}} RT n_i}\right) = RT \ln\left(Z_{\mathrm{mix}} \phi_i\right) = RT(\ln(Z_{\mathrm{mix}}) + \ln(\phi_i)) \tag{S2}$$

where $Z_{\mathrm{mix}} = (PV)/(RTn_{\mathrm{t}})$ is the compressibility factor of the total gas mixture. For the mixture at low pressure P, the Lewis-Randall rule[4] can be applied to approximate the fugacities of species i (f_i) in the mixture in terms of the fugacities of the pure gas of species i ($f_{\mathrm{pure},i}$):

$$f_i \approx y_i f_{\mathrm{pure},i} = \phi_{\mathrm{pure},i} y_i P \tag{S3}$$

where $\phi_{\mathrm{pure},i}$ is the fugacity coefficient of the pure gas of species i at a given T and P. The compressibility factor of the pure solution of species i ($Z_{\mathrm{pure},i}$) can be approximated using the virial expansion (in terms of P)[4]:

$$Z_{\mathrm{pure},i} = \frac{PV}{n_i RT} \approx 1 + B_{2P,i} P \tag{S4}$$

where $B_{2P,i}$ is the second virial coefficient of species i (in the pressure expansion) in units of Pa^{-1}. $\phi_{\mathrm{pure},i}$ is related to $Z_{\mathrm{pure},i}$ and $B_{2P,i}$ via[4]:

$$\ln(\phi_{\text{pure},i}) = \int_0^P \frac{Z_{\text{pure},i} - 1}{p} \mathrm{d}p \approx B_{2P,i} P \tag{S5}$$

Combining Eq. S5 and Eq. S2 results in:

$$\mu^{\text{ex}}_{\text{G},i} \approx RT(\ln(Z_{\text{mix}}) + B_{2P,i} P) \tag{S6}$$

Eq. S6 relates the excess chemical potential of species i to the second virial coefficient of the pure solution of species i and the compressibility factor of the mixture, which can be easily computed using molecular simulations. For small values of $\mu^{\text{ex}}_{\text{G},i}$ (ca. 0.01 kJ/mol), computing $\mu^{\text{ex}}_{\text{G},i}$ directly using molecular simulations is not efficient as long simulations will be needed to reduce the relative error of $\mu^{\text{ex}}_{\text{G},i}$. Eq. S6 can be used as an alternative for predicting $\mu^{\text{ex}}_{\text{G},i}$ as it is easy to compute the second virial coefficient in the gas phase.

The excess chemical potential of the pure gas of species i ($\mu^{\text{ex}}_{\text{G,Pure},i}$) can be predicted using $Z_{\text{pure},i}$ and $B_{2P,i}$ using:

$$\mu^{\text{ex}}_{\text{G,Pure},i} \approx RT(\ln(1 + B_{2P,i} P) + B_{2P,i} P) \approx 2RT B_{2P,i} P \tag{S7}$$

in which the Taylor series expansion of the natural logarithm is used to approximate $\ln(1 + B_{2P,i}P)$ as $B_{2P,i}P$. Note that in this section, we have derived a relation in terms of the pressure-based second virial coefficient. The density-based second virial coefficient (i.e., $B_{2V,i}$ in units of reciprocal density) can also be used to predict $\mu^{\text{ex}}_{\text{G,Pure},i}$. The relation $B_{2P,i} = B_{2V,i}/(RT)$ can be used[4] to rewrite Eq. S7 in terms of $B_{2V,i}$:

$$\mu^{\text{ex}}_{\text{G,Pure},i} \approx 2B_{2V,i} P \tag{S8}$$

In the main text, we use Eq. S8 to compare excess chemical potentials in the gas phase of TIP4P/2005[5] computed in this work (using Monte Carlo simulations) with the reported density-based second virial coefficients of TIP4P/2005 by Rouha *et al.*[6]. The results are discussed in Figure 2 of the main text.

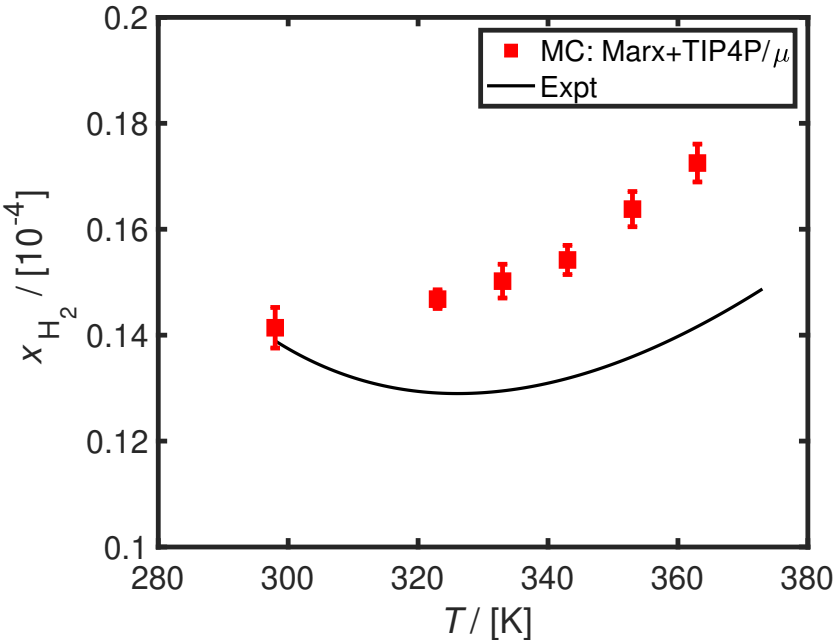

FIG. S1: Computed mole fraction (solubility) of H_2 (x_{H_2}) in pure water using the TIP4P/μ H_2O force field (discussed in the Supporting Information of Ref.[2]) in combination with the Marx[1] H_2 force field as a function of temperature (T) at a H_2 fugacity of 1 bar. The solid line represents the experimental correlation provided by Torín-Ollarves and Trusler[7]. The force field parameters of TIP4P/μ water[2] and Marx H_2 models are listed in Table S1 and S2, respectively.

TABLE S1: Parameters for TIP4P/2005[5] and TIP4P/μ water force fields (discussed in the Supporting Information of Ref.[2]). σ and ϵ are the Lennard-Jones parameters, q are atomic partial charges, and l is the bond length. σ and l are in units of Å, ϵ is in units of kJ/mol, and q is in units of the elementary charge e. In all force fields, the charge on O is on a massless site M, which is equidistant from both H atoms. With the exception of the results shown in Figure S1, the TIP4P/2005 water force field[5] is used for all simulations.

	TIP4P/2005[5]	TIP4P/μ[2]
$\mathrm{H}-\widehat{\mathrm{O}}-\mathrm{H}\,(^{\mathrm{o}})$	104.52	104.52
$l_{\mathrm{O-H}}$	0.9572	0.9572
$l_{\mathrm{O-M}}$	0.1546	0.1546
σ_{OO}	3.1589	3.1589
σ_{HH}	0	0
ϵ_{OO}	0.774908	0.663989
ϵ_{HH}	0	0
q_{O}	0	0
q_{M}	-1.1128	-1.06272
q_{H}	0.5564	0.53136

TABLE S2: Force field parameters for the three-site Marx[1] H_2 model. σ and ϵ are the Lennard-Jones parameters, q is the atomic partial charge, dummy site L is the geometric center of mass, and l is the bond length. σ and l are in units of Å, ϵ is in units of kJ/mol, and q is in units of the elementary charge e.

σ_{LL}	2.958
ϵ_{LL}	0.305141
q_{H}	0.468
q_{L}	-0.936
$l_{\mathrm{H-H}}$	0.74

TABLE S3: Force field parameters for the Madrid-2019[8] Na^+/Cl^- model. σ and ϵ are the Lennard-Jones parameters and q is the atomic partial charge. σ is units of Å, ϵ is in units of kJ/mol, and q is in units of the elementary charge e. O_w refers to the O-atom of water (TIP4P/2005[5] model).

$\sigma_{Na^+Na^+}$	2.21737
$\sigma_{Na^+Cl^-}$	3.00512
$\sigma_{Cl^-Cl^-}$	4.69906
$\sigma_{Na^+O_w}$	2.60838
$\sigma_{Cl^-O_w}$	4.23867
$\epsilon_{Na^+Na^+}$	1.472356
$\epsilon_{Na^+Cl^-}$	1.438894
$\epsilon_{Cl^-Cl^-}$	0.076923
$\epsilon_{Na^+O_w}$	0.793388
$\epsilon_{Cl^-O_w}$	0.061983
q_{Na^+}	0.85
q_{Cl^-}	-0.85

TABLE S4: Force field parameters for the Madrid-Transport[9] K^+ model. σ and ϵ are the Lennard-Jones parameters and q is the atomic partial charge. σ is units of Å, ϵ is in units of kJ/mol, and q is in units of the elementary charge e. O_w refers to the O-atom of water (TIP4P/2005[5] model).

$\sigma_{K^+O_w}$	2.89540
$\sigma_{K^+K^+}$	2.30140
$\epsilon_{K^+K^+}$	1.985740
$\epsilon_{K^+O_w}$	1.400430
q_{K^+}	0.75

TABLE S5: Parameters for the Delft Force Field of OH^- (DFF/OH^-)[10]. OH^- is modeled as a rigid molecule with a bond length of 0.98Å[10]. σ and ϵ are the Lennard-Jones parameters and q is the atomic partial charge. σ is units of Å, ϵ is in units of kJ/mol, and q is in units of the elementary charge e. O represents the oxygen atom and H represents the hydrogen atom of OH^-. The Lorentz-Berthelot mixing rules[11] are used for all atom types.

σ_{OO}	3.65
ϵ_{OO}	0.251
σ_{HH}	1.443
ϵ_{HH}	0.184
q_O	-1.2181
q_H	+0.4681

TABLE S6: The numbers of water molecules and Na^+/Cl^- ions (N) used in Continuous Fractional Component Monte Carlo (CFCMC)[12–16] simulations to compute excess chemical potentials (with respect to the ideal gas reference state) of water and H_2, and activities of water in aqueous NaCl solutions. m refers to the salt molality in units of mol salt / kg water. The average box volume ($\langle V \rangle$) in units of $Å^3$ is shown for each molality at 298 K and 50 bar.

m	N_{H_2O}	N_{Na^+}	N_{Cl^-}	$\langle V \rangle$
0	300	0	0	9019.3
2.03	300	11	11	9374.5
4.07	300	22	22	9773.4
5.92	300	32	32	10152.8

TABLE S7: The numbers of water molecules and K^+/OH^- ions (N) used in Continuous Fractional Component Monte Carlo (CFCMC)[12–16] simulations to compute excess chemical potentials (with respect to the ideal gas reference state) of water and H_2, and activities of water in aqueous KOH solutions. m refers to the salt molality in units of mol salt / kg water. The average box volume ($\langle V \rangle$) in units of $Å^3$ is shown for each molality at 298 K and 50 bar.

m	N_{H_2O}	N_{Na^+}	N_{Cl^-}	$\langle V \rangle$
0	300	0	0	9019.3
2.03	300	11	11	9192.4
4.07	300	22	22	9465.1
5.92	300	32	32	9749.6
7.96	300	43	43	10096.7

TABLE S8: Results for the computed Vapor-Liquid Equilibria (VLE) of H_2 and aqueous NaCl solutions at different temperatures (T in units of K) and NaCl molalities (m in units of mol NaCl / kg water) at 50 bar. The liquid densities (ρ_L in units of kg m^{-3}), activities of water (i.e., $a_{H_2O} = \gamma_{H_2O} x_{H_2O}$, where γ_{H_2O} and x_{H_2O} are the activity coefficient and the mole fraction of water in the liquid phase, respectively), fugacity coefficients of water (ϕ_{H_2O}) and H_2 (ϕ_{H_2}) in the gas phase, mole fraction of water in the gas phase (y_{H_2O}), and the mole fraction (i.e., solubility) of H_2 in the liquid phase (x_{H_2}) are shown at different T and m. The computational methodology used (including the choice of force fields) is discussed in Section II of the main text. σ_x are the computed standard deviations of quantity x.

T	m	ρ_L	σ_{ρ_L}	a_{H_2O}	$\sigma_{a_{H_2O}}$	ϕ_{H_2O}	ϕ_{H_2}	y_{H_2O}	$\sigma_{y_{H_2O}}$	x_{H_2}	$\sigma_{x_{H_2}}$
298	2.04	1088.0	1.7	0.945	0.024	0.942	1.030	0.00066	0.00004	0.000420	0.000044
298	4.07	1164.0	1.6	0.885	0.026	0.942	1.030	0.00058	0.00003	0.000262	0.000011
298	5.92	1227.0	1.8	0.845	0.031	0.942	1.030	0.00055	0.00001	0.000199	0.000007
298	7.96	1286.0	2.1	0.798	0.016	0.942	1.030	0.00053	0.00003	0.000150	0.000011
323	2.04	1074.0	1.5	0.956	0.032	0.955	1.028	0.00264	0.00031	0.000409	0.000015
323	4.07	1150.0	1.3	0.918	0.018	0.956	1.028	0.00240	0.00006	0.000307	0.000016
323	5.92	1210.0	1.6	0.872	0.01	0.956	1.028	0.00226	0.00003	0.000213	0.000024
323	7.96	1268.0	1.2	0.805	0.025	0.956	1.028	0.00217	0.00013	0.000155	0.000014
363	2.04	1048.0	0.8	0.955	0.01	0.967	1.026	0.01455	0.00043	0.000458	0.000027
363	4.07	1121.0	1.2	0.908	0.006	0.968	1.026	0.01360	0.00019	0.000343	0.000006
363	5.92	1180.0	1.0	0.861	0.006	0.968	1.026	0.01304	0.00027	0.000274	0.000018
363	7.96	1238.0	1.1	0.816	0.011	0.968	1.026	0.01237	0.00015	0.000230	0.000010
393	2.04	1024.0	0.8	0.954	0.005	0.969	1.025	0.04091	0.00083	0.000543	0.000006
393	4.07	1096.0	0.9	0.913	0.004	0.969	1.025	0.03890	0.00061	0.000415	0.000021
393	5.92	1155.0	1.0	0.873	0.015	0.969	1.025	0.03796	0.00021	0.000325	0.000015
393	7.96	1213.0	0.8	0.825	0.005	0.970	1.024	0.03513	0.00051	0.000269	0.000011
423	2.04	996.7	0.9	0.957	0.005	0.964	1.024	0.09749	0.00176	0.000619	0.000023
423	4.07	1070.0	1.0	0.91	0.007	0.965	1.024	0.09175	0.00071	0.000481	0.000016
423	5.92	1128.0	1.2	0.875	0.006	0.966	1.024	0.08881	0.00186	0.000394	0.000015
423	7.96	1186.0	1.6	0.829	0.002	0.967	1.024	0.08368	0.00120	0.000323	0.000013

TABLE S9: Results for the computed Vapor-Liquid Equilibria (VLE) of H_2 and aqueous KOH solutions at different temperatures (T in units of K) and KOH molalities (m in units of mol KOH / kg water) at 50 bar. The liquid densities (ρ_L in units of kg m^{-3}), activities of water (i.e., $a_{H_2O} = \gamma_{H_2O} x_{H_2O}$, where γ_{H_2O} and x_{H_2O} are the activity coefficient and the mole fraction of water in the liquid phase, respectively), fugacity coefficients of water (ϕ_{H_2O}) and H_2 (ϕ_{H_2}) in the gas phase, mole fraction of water in the gas phase (y_{H_2O}), and the mole fraction (i.e., solubility) of H_2 in the liquid phase (x_{H_2}) are shown at different T and m. The computational methodology used (including the choice of force fields) is discussed in Section II of the main text. σ_x are the computed standard deviations of quantity x.

T	P	m	ρ_L	σ_{ρ_L}	a_{H_2O}	$\sigma_{a_{H_2O}}$	ϕ_{H_2O}	ϕ_{H_2}	y_{H_2O}	$\sigma_{y_{H_2O}}$	x_{H_2}	$\sigma_{x_{H_2}}$
298	50	0.00	995.2	1.2	1.000	0.000	0.942	1.030	0.00067	0.00002	0.000701	0.000051
298	50	2.04	1072.0	1.1	0.918	0.013	0.942	1.030	0.00062	0.00002	0.000488	0.000014
298	50	4.07	1137.0	1.6	0.837	0.024	0.942	1.030	0.00057	0.00001	0.000344	0.000031
298	50	5.92	1190.0	1.6	0.786	0.024	0.942	1.030	0.00054	0.00002	0.000249	0.000015
323	50	0.00	985.7	1.0	1.000	0.000	0.955	1.028	0.00260	0.00006	0.000656	0.000021
323	50	2.04	1058.0	0.9	0.935	0.022	0.955	1.028	0.00244	0.00007	0.000471	0.000021
323	50	4.07	1122.0	1.0	0.855	0.021	0.956	1.028	0.00227	0.00010	0.000351	0.000030
323	50	5.92	1173.0	1.2	0.776	0.008	0.956	1.028	0.00205	0.00005	0.000282	0.000014
363	50	0.00	961.3	0.6	1.000	0.000	0.967	1.026	0.01516	0.00011	0.000692	0.000021
363	50	2.04	1032.0	0.8	0.935	0.008	0.967	1.026	0.01420	0.00028	0.000519	0.000011
363	50	4.07	1093.0	0.9	0.859	0.003	0.968	1.026	0.01302	0.00011	0.000417	0.000008
363	50	5.92	1142.0	0.8	0.788	0.009	0.968	1.026	0.01170	0.00015	0.000340	0.000011
393	50	0.00	937.9	0.6	1.000	0.000	0.968	1.025	0.04249	0.00042	0.000760	0.000017
393	50	2.04	1008.0	0.6	0.934	0.011	0.969	1.025	0.04017	0.00068	0.000594	0.000010
393	50	4.07	1069.0	0.7	0.860	0.008	0.970	1.024	0.03672	0.00031	0.000480	0.000013
393	50	5.92	1117.0	0.7	0.793	0.007	0.971	1.024	0.03344	0.00056	0.000415	0.000012
423	50	0.00	910.0	0.6	1.000	0.000	0.963	1.024	0.10110	0.00113	0.000866	0.000014
423	50	2.04	981.3	0.6	0.932	0.012	0.965	1.024	0.09410	0.00039	0.000698	0.000019
423	50	4.07	1042.0	0.5	0.862	0.004	0.966	1.024	0.08724	0.00134	0.000567	0.000020
423	50	5.92	1090.0	0.8	0.795	0.003	0.968	1.024	0.07985	0.00127	0.000475	0.000011

TABLE S10: Results for the computed Vapor-Liquid Equilibria (VLE) of H_2 and water (salt molality of 0 mol salt / kg water) at different temperatures (T in units of K) and pressures (P in units of bar). The liquid densities (ρ_L in units of kg m^{-3}), fugacity coefficients of water (ϕ_{H_2O}) and H_2 (ϕ_{H_2}) in the gas phase, mole fraction of water in the gas phase (y_{H_2O}), and the mole fraction (i.e., solubility) of H_2 in the liquid phase (x_{H_2}) are shown at different T and P. ϕ_{H_2O}, ϕ_{H_2}, y_{H_2O}, and x_{H_2} are unitless. The computational methodology used (including the choice of force fields) is discussed in Section II of the main text. σ_x are the computed standard deviations of quantity x.

T	P	ρ_L	σ_{ρ_L}	ϕ_{H_2O}	ϕ_{H_2}	y_{H_2O}	$\sigma_{y_{H_2O}}$	x_{H_2}	$\sigma_{x_{H_2}}$
298	10	993.6	1.0	0.987	1.006	0.003147	0.000114	0.000141	0.000010
298	100	997.1	1.4	0.897	1.061	0.000361	0.000011	0.001412	0.000107
298	500	1015.0	1.1	0.779	1.362	0.000114	0.000007	0.006602	0.000550
323	10	983.0	0.7	0.989	1.006	0.012500	0.000304	0.000131	0.000005
323	100	987.8	1.3	0.921	1.057	0.001434	0.000057	0.001264	0.000041
323	200	991.9	1.0	0.874	1.120	0.000795	0.000018	0.002615	0.000080
323	500	1005.0	1.2	0.845	1.336	0.000400	0.000008	0.005849	0.000132
363	10	959.2	0.6	0.989	1.005	0.071760	0.001004	0.000131	0.000005
363	100	963.9	0.6	0.946	1.053	0.008018	0.000126	0.001395	0.000041
363	500	982.0	0.7	0.923	1.300	0.002069	0.000027	0.006215	0.000086
423	10	908.0	0.6	0.977	1.013	0.488100	0.002132	0.000100	0.000002
423	100	913.3	0.5	0.952	1.047	0.052700	0.000646	0.001823	0.000047
423	500	935.1	0.5	0.978	1.258	0.012750	0.000083	0.008072	0.000185

TABLE S11: Results for the computed Vapor-Liquid Equilibria (VLE) of H_2 and aqueous NaCl solutions (salt molality of 5.92 mol NaCl / kg water) at different temperatures (T in units of K) and pressures (P in units of bar). The liquid densities (ρ_L in units of kg m^{-3}), fugacity coefficients of water (ϕ_{H_2O}) and H_2 (ϕ_{H_2}) in the gas phase, mole fraction of water in the gas phase (y_{H_2O}), and the mole fraction (i.e., solubility) of H_2 in the liquid phase (x_{H_2}) are shown at different T and P. ϕ_{H_2O}, ϕ_{H_2}, y_{H_2O}, and x_{H_2} are unitless. The computational methodology used (including the choice of force fields) is discussed in Section II of the main text. σ_x are the computed standard deviations of quantity x.

T	P	ρ_L	σ_{ρ_L}	ϕ_{H_2O}	ϕ_{H_2}	y_{H_2O}	$\sigma_{y_{H_2O}}$	x_{H_2}	$\sigma_{x_{H_2}}$
298	10	1188.0	2.3	0.987	1.006	0.002347	0.000111	0.000055	0.000007
298	100	1191.0	1.5	0.897	1.061	0.000276	0.000008	0.000537	0.000049
298	200	1195.0	1.6	0.833	1.127	0.000155	0.000007	0.001015	0.000133
298	500	1204.0	1.4	0.779	1.362	0.000087	0.000004	0.002471	0.000267
323	10	1171.0	1.2	0.990	1.006	0.009740	0.000474	0.000061	0.000002
323	100	1175.0	1.2	0.921	1.057	0.001088	0.000018	0.000573	0.000011
323	200	1178.0	1.5	0.874	1.120	0.000633	0.000022	0.001091	0.000046
323	500	1188.0	1.1	0.845	1.336	0.000315	0.000012	0.002640	0.000138
363	10	1141.0	1.0	0.990	1.005	0.056800	0.001464	0.000070	0.000003
363	100	1144.0	1.4	0.947	1.053	0.006175	0.000139	0.000676	0.000010
363	200	1148.0	0.9	0.920	1.109	0.003383	0.000084	0.001315	0.000098
363	500	1159.0	0.9	0.924	1.300	0.001641	0.000049	0.003242	0.000101
423	10	1088.0	1.2	0.982	1.008	0.383900	0.005608	0.000067	0.000002
423	100	1093.0	0.9	0.957	1.047	0.041370	0.000683	0.000992	0.000023
423	200	1097.0	0.8	0.948	1.096	0.022280	0.000327	0.001959	0.000069
423	500	1111.0	0.9	0.986	1.258	0.009899	0.000111	0.004555	0.000083

TABLE S12: Results for the computed Vapor-Liquid Equilibria (VLE) of H_2 and aqueous KOH solutions (salt molality of 4.07 mol KOH / kg water) at different temperatures (T in units of K) and pressures (P in units of bar). The liquid densities (ρ_L in units of kg m^{-3}), fugacity coefficients of water (ϕ_{H_2O}) and H_2 (ϕ_{H_2}) in the gas phase, mole fraction of water in the gas phase (y_{H_2O}), and the mole fraction (i.e., solubility) of H_2 in the liquid phase (x_{H_2}) are shown at different T and P. ϕ_{H_2O}, ϕ_{H_2}, y_{H_2O}, and x_{H_2} are unitless. The computational methodology used (including the choice of force fields) is discussed in Section II of the main text. σ_x are the computed standard deviations of quantity x.

T	P	ρ_L	σ_{ρ_L}	ϕ_{H_2O}	ϕ_{H_2}	y_{H_2O}	$\sigma_{y_{H_2O}}$	x_{H_2}	$\sigma_{x_{H_2}}$
298	10	1164.0	2.7	0.987	1.006	0.002837	0.000095	0.000054	0.000005
298	100	1167.0	1.7	0.897	1.061	0.000328	0.000011	0.000529	0.000072
298	200	1171.0	1.4	0.833	1.127	0.000193	0.000015	0.001079	0.000138
298	500	1180.0	2.2	0.779	1.362	0.000101	0.000004	0.002592	0.000372
363	10	1120.0	1.1	0.990	1.005	0.064660	0.001430	0.000068	0.000003
363	100	1123.0	1.2	0.947	1.053	0.007195	0.000167	0.000713	0.000036
363	200	1127.0	1.0	0.919	1.109	0.003905	0.000086	0.001405	0.000078
363	500	1139.0	1.5	0.923	1.300	0.001875	0.000023	0.003233	0.000201
423	10	1068.0	1.1	0.979	1.010	0.443800	0.007219	0.000061	0.000002
423	100	1072.0	1.0	0.954	1.047	0.047580	0.000498	0.000972	0.000032
423	200	1077.0	0.9	0.945	1.096	0.025780	0.000224	0.001949	0.000057
423	500	1090.0	1.0	0.981	1.258	0.011690	0.000146	0.004475	0.000181

TABLE S13: Results for the computed Vapor-Liquid Equilibria (VLE) of H_2 and aqueous KOH solutions (salt molality of 7.96 mol KOH / kg water) at different temperatures (T in units of K) and pressures (P in units of bar). The liquid densities (ρ_L in units of kg m^{-3}), fugacity coefficients of water (ϕ_{H_2O}) and H_2 (ϕ_{H_2}) in the gas phase, mole fraction of water in the gas phase (y_{H_2O}), and the mole fraction (i.e., solubility) of H_2 in the liquid phase (x_{H_2}) are shown at different T and P. ϕ_{H_2O}, ϕ_{H_2}, y_{H_2O}, and x_{H_2} are unitless. The computational methodology used (including the choice of force fields) is discussed in Section II of the main text. σ_x are the computed standard deviations of quantity x.

T	P	ρ_L	σ_{ρ_L}	ϕ_{H_2O}	ϕ_{H_2}	y_{H_2O}	$\sigma_{y_{H_2O}}$	x_{H_2}	$\sigma_{x_{H_2}}$
298	10	1285.0	1.6	0.987	1.006	0.002473	0.000057	0.000031	0.000003
298	100	1288.0	1.7	0.897	1.061	0.000291	0.000020	0.000311	0.000025
298	200	1291.0	1.9	0.833	1.127	0.000167	0.000010	0.000558	0.000050
298	500	1300.0	1.9	0.779	1.362	0.000089	0.000004	0.001339	0.000038
323	10	1267.0	1.2	0.990	1.006	0.009964	0.000155	0.000037	0.000003
323	100	1270.0	1.2	0.921	1.057	0.001150	0.000029	0.000330	0.000028
323	200	1272.0	1.9	0.874	1.120	0.000619	0.000026	0.000684	0.000054
323	500	1283.0	1.1	0.845	1.336	0.000327	0.000017	0.001489	0.000073
363	10	1236.0	1.2	0.990	1.005	0.058360	0.001449	0.000040	0.000001
363	100	1239.0	1.1	0.947	1.053	0.006404	0.000098	0.000447	0.000012
363	200	1243.0	1.2	0.920	1.109	0.003521	0.000033	0.000854	0.000026
363	500	1253.0	1.2	0.924	1.300	0.001676	0.000053	0.002061	0.000062
423	10	1185.0	0.8	0.981	1.009	0.405000	0.002448	0.000042	0.000002
423	100	1189.0	0.9	0.956	1.047	0.043380	0.000465	0.000662	0.000023
423	200	1192.0	1.0	0.947	1.096	0.023320	0.000617	0.001354	0.000087
423	500	1204.0	0.8	0.984	1.258	0.010570	0.000067	0.003102	0.000072

REFERENCES

[1]D. Marx and P. Nielaba, Phys. Rev. A **45**, 8968 (1992).

[2]A. Rahbari, J. C. Garcia-Navarro, M. Ramdin, L. J. P. van den Broeke, O. A. Moultos, D. Dubbeldam, and T. J. H. Vlugt, J. Chem. Eng. Data **66**, 2071 (2021).

[3]A. Rahbari, J. Brenkman, R. Hens, M. Ramdin, L. J. V. D. Broeke, R. Schoon, R. Henkes, O. A. Moultos, and T. J. H. Vlugt, J. Chem. Eng. Data **64**, 4103 (2019).

[4]J. M. Prausnitz, R. N. Lichtenthaler, and E. G. De Azevedo, *Molecular thermodynamics of fluid-phase equilibria* (Pearson Education, 1998).

[5]J. L. Abascal and C. Vega, J. Chem. Phys. **123**, 234505 (2005).

[6]M. Rouha, I. Nezbeda, J. Hrubỳ, and F. Moučka, J. Mol. Liq. **270**, 81 (2018).

[7]G. A. Torín-Ollarves and J. M. Trusler, Fluid Ph. Equilib. **539**, 113025 (2021).

[8]I. M. Zeron, J. L. F. Abascal, and C. Vega, J. Chem. Phys. **151**, 104501 (2019).

[9]S. Blazquez, M. M. Conde, and C. A. Vega, J. Chem. Phys. **158**, 054505 (2023).

[10]P. Habibi, A. Rahbari, S. Blazquez, C. Vega, P. Dey, T. J. H. Vlugt, and O. A. Moultos, J. Phys. Chem. B **126**, 9376 (2022).

[11]D. Frenkel and B. Smit, *Understanding Molecular Simulation: from Algorithms to Applications*, 3rd ed. (Elsevier, San Diego, 2023).

[12]A. Rahbari, R. Hens, M. Ramdin, O. A. Moultos, D. Dubbeldam, and T. J. H. Vlugt, Mol. Simulat. **47**, 804 (2021).

[13]W. Shi and E. J. Maginn, J. Chem. Theory Comput. **3**, 1451 (2007).

[14]W. Shi and E. J. Maginn, J. Comput. Chem. **29**, 2520 (2008).

[15]R. Hens, A. Rahbari, S. Caro-Ortiz, N. Dawass, M. Erdős, A. Poursaeidesfahani, H. S. Salehi, A. T. Celebi, M. Ramdin, O. A. Moultos, D. Dubbeldam, and T. J. H. Vlugt, J. Chem. Inf. Model. **60**, 2678 (2020).

[16]H. M. Polat, H. S. Salehi, R. Hens, D. O. Wasik, A. Rahbari, F. de Meyer, C. Houriez, C. Coquelet, S. Calero, D. Dubbeldam, O. A. Moultos, and T. J. H. Vlugt, J. Chem. Inf. Model. **61**, 3752 (2021).